Energies **2009**, *2*, 789-804; doi:10.3390/en20300789

OPEN ACCESS

energies

ISSN 1996-1073

www.mdpi.com/journal/energies

Article

Methanol Electro-Oxidation on Pt-Ru Alloy Nanoparticles Supported on Carbon Nanotubes

Liang Li [1,#] and Yangchuan Xing [1,*]

[1] Department of Chemical and Biological Engineering, Missouri University of Science and Technology, Rolla, MO 65409, USA

[#] Current address: Northeastern University, Boston, MA 02148, USA; E-Mail: l.li@neu.edu.

* Author to whom correspondence should be addressed; E-Mail: xingy@mst.edu; Tel.: +1-573-341-6772; Fax: +1-573-341-4377.

Received: 5 August 2009 / Accepted: 11 September 2009 / Published: 16 September 2009

Abstract: Carbon nanotubes (CNTs) have been investigated in recent years as a catalyst support for proton exchange membrane fuel cells. Improved catalyst activities were observed and attributed to metal-support interactions. We report a study on the kinetics of methanol electro-oxidation on CNT supported Pt-Ru alloy nanoparticles. Alloy catalysts with different compositions, $Pt_{53}Ru_{47}$/CNT, $Pt_{69}Ru_{31}$/CNT and $Pt_{77}Ru_{23}$/CNT, were prepared and investigated in detail. Experiments were conducted at various temperatures, electrode potentials, and methanol concentrations. It was found that the reaction order of methanol electro-oxidation on the PtRu/CNT catalysts was consistent with what has been reported for PtRu alloys with a value of 0.5 in methanol concentrations. However, the electro-oxidation reaction on the PtRu/CNT catalysts displayed much lower activation energies than that on the Pt-Ru alloy catalysts unsupported or supported on carbon black (PtRu/CB). This study provides an overall kinetic evaluation of the PtRu/CNT catalysts and further demonstrates the beneficial role of CNTs.

Keywords: PtRu catalysts; methanol electro-oxidation; carbon nanotubes; fuel cells

1. Introduction

There has been a constant search for catalysts that are efficient in the electro-oxidation of methanol in direct methanol fuel cells (DMFCs) for portable electronic devices. Electro-oxidation of methanol is

a complex process involving the exchange of six electrons and formation of numerous intermediates [1]. The reactions often involve formic acid, methylformate or formaldehyde as intermediates during the oxidation process [2-4]. The reactions are slow and require active catalytic sites for adsorption and oxidation of methanol, as well as oxidation and desorption of the adsorbed intermediates [5].

The most studied catalysts for methanol electro-oxidation are Pt-Ru alloys [2-4,8,9]. It has been found that Pt-Ru alloy catalysts generally have high activity, which was attributed to the ability of the Ru in the alloys to form active oxygen species (-OH) at low electrode potentials (~0.2V) that can remove poisonous carbon monoxide on the Pt sites [6,7]. The enhanced activity was also attributed to the change of electronic structures of Pt when the more electronegative Ru is alloyed [10-13]. Gasteiger *et al.* found that Pt-Ru alloy with a Ru surface composition of *ca.* 50% atomic percent (*i.e.*, Pt to Ru atomic ratio is 1:1) was the most active, and displayed a strong synergistic effect in methanol electro-oxidation [8]. Takasu *et al.* reported that supported, high surface area Pt-Ru catalysts on carbon black showed a maximum in both mass and specific activities with about 50% Ru at 60 ºC in the potential range of 0.4~0.5 V [9]. It was also observed that the distributions of Pt and Ru sites at the atomic level can substantially affect the catalyst activity [2,8].

Recent efforts have been made to use carbon nanotubes (CNTs) as supports for Pt-Ru alloy catalysts. It was found that CNTs, which have definitive graphitic surface structures, can enhance the catalyst activity [14-24]. We have recently demonstrated that CNT-supported Pt-Ru alloy catalysts (PtRu/CNT) with various atomic compositions have higher catalytic activity than the corresponding Pt-Ru catalyst supported on carbon black [24]. The CNT-supported catalysts with a Pt to Ru ratio close to 1:1 showed the best catalytic activity and stability. Catalysts with other Pt to Ru ratios showed higher activity, but their stability was not as good.

Despite PtRu/CNT being a good catalyst, there has been a lack of kinetic studies of the catalyst for methanol electro-oxidation. The current work focuses on understanding the kinetics of the PtRu/CNT catalysts in the electro-oxidation of methanol. Catalysts with different atomic ratios, namely, $Pt_{53}Ru_{47}$/CNT, $Pt_{69}Ru_{31}$/CNT and $Pt_{77}Ru_{23}$/CNT, were prepared and investigated in detail. Experiments were performed at various temperatures, electrode potentials, and methanol concentrations. Several kinetic parameters were obtained, including Tafel slopes, activation energies, and reaction orders.

2. Experimental Section

Deposition of Pt-Ru nanoparticles on multi-walled CNTs (95% purity, NanoLab, Inc.) was achieved by reduction of metal salts with ethylene glycol [25,26]. The metal loading of the catalysts was preset at 20wt% based on the amount of metal salt precursors used. The details of the Pt-Ru catalyst preparation process can be found in a previous paper [24]. Briefly, Pt and Ru salt precursors, K_2PtCl_4 and K_2RuCl_5 (Alfa Aesar), were mixed with sonochemically functionalized CNTs in an ethylene glycol-water solution [27]. Reduction reactions were carried out under reflux conditions for 2 hours with continuous magnetic stirring. Highly dispersed Pt-Ru alloy nanoparticles with three alloy compositions, $Pt_{53}Ru_{47}$, $Pt_{69}Ru_{31}$, and $Pt_{77}Ru_{23}$, were made uniformly on the external walls of the CNTs. The average particle sizes are 2~3 nm [24].

All of the electrochemical measurements were conducted in an electrochemical cell in a Faraday cage (C3 Cell, Bioanalytical Sciences). Potentials of the working electrode were measured against a Ag/AgCl reference electrode, and a platinum wire was used as the counter electrode. A thin film electrode technique was used to prepare the working electrode [28]. A glassy carbon disk (3 mm in diameter, or 0.071 cm^2 in area) was polished to a mirror finish with 0.05 μm alumina pastes before each measurement, and served as the substrate for the PtRu/CNT catalysts. Aqueous suspensions of the catalysts with a concentration of 1.0 mg/mL were made by ultrasonically dispersing 5 mg of a PtRu/CNT catalyst in 5 mL deionized water. A 30 μL aliquot of the suspension was put onto the glassy carbon substrate. After evaporation of the water, 10 μL of a Nafion solution (5 wt%, Alfa Aesar) was put on top of the catalyst, acting as both a binder and an electrolyte.

Electro-oxidation of methanol was performed in 1.0 M H_2SO_4 containing 2.0 M methanol. The solution was prepared with high-purity water (Millipore, 18.2 MΩ resistance). Electrochemical experiments were conducted in a jacked beaker (100 mL) with a Teflon cap that has holes to fit electrodes and a purging gas line. A constant temperature circulator (Polystat, Cole Parmer) was used to keep the experiments running at a preset temperature. During the experiments, ultrahigh purity Ar was introduced into the electrochemical cell above the solution as a protection atmosphere. All potentials reported in this paper have been converted to potentials relative to the reversed hydrogen electrode (RHE) potential, unless otherwise noted.

3. Results and Discussion

3.1. Cyclic Voltammetry

Cyclic voltammetry (CV) of the Pt-Ru alloy catalysts was performed at temperatures of 25, 35, 45 and 60 ºC. The scan rate was 20 mV/s for all experiments, with potentials ranging from 0 to 0.75 V. The thin film electrode was immersed in the electrolyte solution and the potential was cycled several times until a steady-state voltammogram was obtained (6~8 cycles). Typical polarization curves in the electro-oxidation of methanol are shown in Figure 1(a) for the $Pt_{53}Ru_{47}$/CNT catalyst. It can be seen that methanol electro-oxidation occurred at all temperatures, but the oxidation currents were significantly enhanced at high temperatures. In the meantime, there was a negative shift of the onset oxidation potentials (Table 1). For example, for $Pt_{53}Ru_{47}$/CNT, the peak current density at 60 ºC was 2.8 times that at 25 ºC, and the onset potential showed a much lower value at 215 mV as compared to 253 mV at 25 ºC. The results indicated that methanol electro-oxidation is thermally activated in the temperature ranges of this study. This is consistent with the results of Arico *et al.* [29] who have reported that Pt-Ru catalysts characterized by a high degree of alloying and metallic behavior on the surface appeared to be more active towards methanol electro-oxidation at higher temperatures. At each temperature, the sequence of the peak current density [Figure 1(b)] showed the same order as observed in a previous work at room temperature [24], implying that the mechanisms at all temperatures are similar.

Table 1. Tafel slopes and onset potentials of the PtRu/CNT catalysts for methanol electro-oxidation at 25 ºC and 60 ºC.

Catalysts	Onset potential (mV)		Tafel slope (mV dec^{-1})	
	25 ºC	60 ºC	25 ºC	60 ºC
$Pt_{53}Ru_{47}$/CNT	253	215	98.8	97.8
$Pt_{69}Ru_{31}$/CNT	272	240	101.3	105.7
$Pt_{77}Ru_{23}$/CNT	262	230	101.1	105.5

Figure 1. (a) Cyclic voltammograms of methanol electro-oxidation on $Pt_{53}Ru_{47}$/CNT with elevated temperatures. (b) Cyclic voltammograms of methanol electro-oxidation on different PtRu/CNT catalysts at 60 ºC.

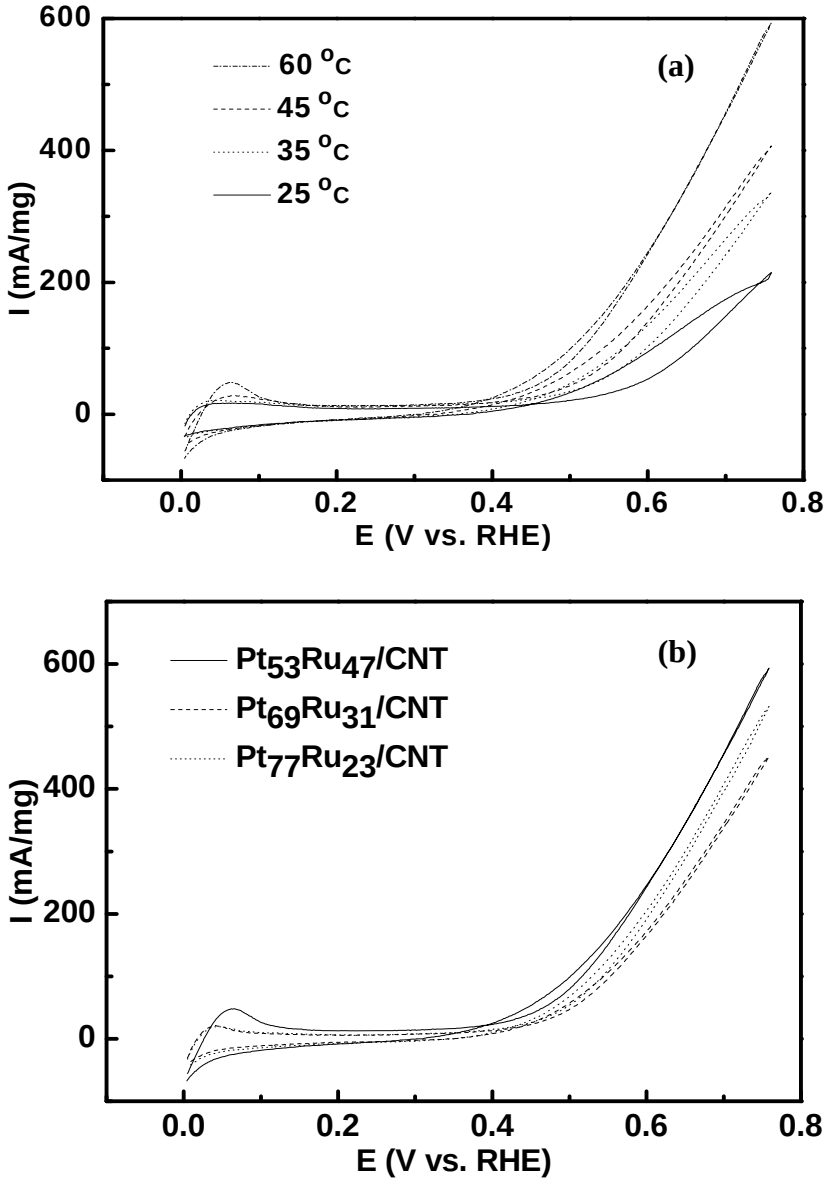

A major reaction pathway for methanol electro-oxidation on Pt-Ru alloys at room temperature was previously proposed, which was primarily based on the balance between initial adsorptive dehydrogenation of methanol and subsequent oxidative removal of dehydrogenation fragments [30,31]. The first step is methanol adsorption, followed by methanol dehydrogenation and formation of adsorbed methanolic residues (CO) on Pt surface, which are both intermediates and surface "poisons".

$$Pt + CH_3OH \rightarrow Pt - CH_3OH_{ads} \rightarrow Pt - CO_{ads} + 4H^+ + 4e \quad (1)$$

On the electrode surface, the removal of CO_{ads} at Pt sites is believed to proceed though the reaction of chemisorbed CO with chemisorbed hydroxyl species (OH_{ads}). At an appropriate electrode potential (*ca.* 0.2 V, significantly lower than that on pure Pt, >0.5 V), water discharging occurs on Ru sites with the formation of Ru-OH groups [32]:

$$Ru + H_2O \rightarrow Ru - OH_{ads} + H^+ + e \quad (2)$$

The final step is the reaction of OH_{ads} groups with neighboring methanolic residues adsorbed on Pt sites to give carbon dioxide:

$$Pt - CO_{ads} + Ru - OH_{ads} \rightarrow Pt + Ru + CO_2 + H^+ + e \quad (3)$$

The enhancement in methanol electro-oxidation at high temperatures may be attributed to the increase in OH adsorption and catalytic activity of Ru. Choi *et al.* [33] reported that elevation in temperatures accelerates the OH adsorption on the Pt-Ru alloy surface. As a result, the rate of CO oxidation to CO_2 on the Pt surface is accelerated since OH was able to be adsorbed on the Ru surface at a lower potential. The negative shift of the onset potentials in our experiments was possibly related to the enhancement of OH_{ads} formation of Equation 2 [34]. Consequently, easier adsorption of OH at higher temperatures resulted in higher electro-oxidation current densities and lower onset potentials. At low temperatures only Pt was found to be active towards methanol dehydrogenation which is a highly thermally activated process on the Ru sites. Hence, Ru sites can only serve for the removal of carbonaceous intermediates and play no role in the dehydrogenation process at low temperatures [8]. However, as the temperature increases, methanol dehydrogenation can occur also on Ru sites. It has been reported that even pure Ru electrode showed some catalytic activity for methanol oxidation at above 40 ºC [8,35]. It is noted that, although at high temperatures Ru can participate in methanol chemisorption and dehydrogenation, the chemisorption energy of oxygen species on Ru surface binding through Ru-O is so high that it inhibits Ru sites from being covered by methanolic residues binding through Ru-C [36]. Consequently, the Ru sites can still suitably adsorb OH groups at high temperatures.

3.2. Bulter-Volmer Plot (Tafel Plot)

The Bulter-Volmer plots (the Tafel range) were derived from the steady-state oxidation experiments obtained potentiostatically with a fixed delay of five minutes at each potential, in the range from 0.35 to 0.8 V (potential steps of 50 mV) [37,38]. The Tafel plots for methanol electro-oxidation at 25 ºC and 60 ºC for the catalysts are shown in Figure 2. Different values of Tafel slope (*i.e.* change in overpotential per decade change in current density) have been reported in the literature. Tafel slopes of 120 mV dec^{-1} on Pt-Ru in Nafion membrane and 110 mV dec^{-1} for PtRu/CB catalysts at 25 ºC were

reported [38,39]; values of 180-195 mV dec^{-1} were reported for bulk Pt-Ru alloy and PtRu/CB catalysts at 60 ºC [8,40]; a value of 132 mV dec^{-1} was reported for Pt-Ru black with a Pt to Ru atomic ratio of 1:1 [1]. It has been suggested that the term "Tafel slope" in the case of the methanol electro-oxidation does not carry its usual sense, since straight lines of *E* vs. log *I* are generally not observed [8].

Figure 2. Tafel plots for methanol electro-oxidation on the PtRu/CNT catalysts.

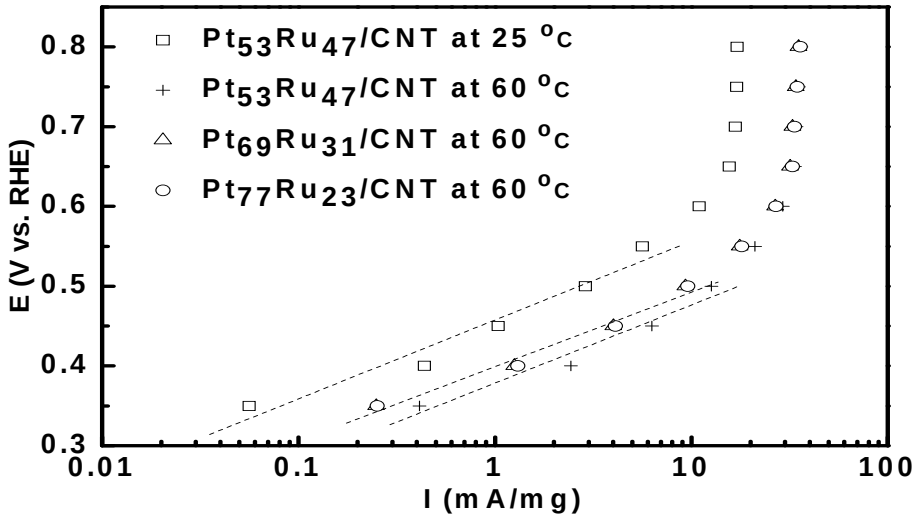

As seen from Figure 2, it is apparent that the Tafel plots can be fitted with two lines that intersect at approximately 0.6 V for all catalysts, with the linear part of the Bulter-Volmer plot at <0.6 V and the deviation from the Bulter-Volmer linearity >0.6 V (*i.e.* where the rate of current increase decelerates with the increase in potential). In the lower potential region (<0.6 V), all the samples showed similar slopes of *ca*. 100 mV dec^{-1}, indicating identical kinetic behaviors. At potentials above 0.6 V, the slope of *E* vs. log *I* curves increased substantially. Since the limiting currents are not mass transfer controlled and they can not be enhanced by changing the rotating speed of the electrode, there must be formation of new adsorbed intermediates. Jusys *et al.* have reported detection of methyl formate in this potential region [3]. They observed that the predominant reaction below 0.6 V corresponds to methanol dehydrogenation, while the predominant process above 0.6 V corresponds to CO oxidation. Thus, the methanol dehydrogenation activities for all catalysts are similar in the low potential range, where the CO oxidation may be affected by the number of neighboring Ru sites. The linear region of the Tafel plots was found to be within the low potential range for all catalysts at 25 ºC and 60 ºC (Figure 2), giving Tafel slopes of *ca.* 100 mV dec^{-1} (Table 1). The similarity among all the catalysts indicates that the reaction mechanism is the same within the experimental temperature ranges despite of different compositions of the catalysts, and the bifunctional mechanism discussed in section 3.1 is appropriate to interpret the methanol electro-oxidation. However, $Pt_{53}Ru_{47}$/CNT catalyst is the most active.

Methanol electro-oxidation has been known to be sensitive to the surface structures of catalysts. The catalytic activity of Pt-Ru catalysts toward methanol electro-oxidation is maximized with the presence of (111) crystallographic planes, and the methanolic CO (surface poisoning) formation is the

slowest on (111) planes in acidic electrolytes [41,42]. Gasteiger, *et al.* found that the balance between the rate of methanol adsorption and the rate of oxidative removal of dehydrogenated fragments determines the activities of Pt-Ru catalysts with different Ru compositions [30]. In our previous study [24] the $Pt_{53}Ru_{47}$/CNT catalyst was shown to have the highest intensity of (111) planes, justifying that it has the highest rate of methanol oxidation mostly via a non-CO path to form CO_2 and the slowest rate of CO formation. This catalyst therefore should have the highest catalytic activity and the best stability among the tested catalysts.

3.3. Potentiostatic Methanol Oxidation on PtRu/CNT

Current *vs.* time measurements at constant potential with different temperatures were carried out to obtain activation energies that can provide information for the fundamental mechanisms. Potentiostatic methanol oxidation was performed at different temperatures of 25, 35, 45 and 60 ºC. Two potentials, 0.4 and 0.5 V, were applied for 1,800 s (30 min). In previous research, higher potentials (from about 0.45 to 0.7 V) have assigned to the limiting current region and lower potentials (from 0.2 to about 0.45 V) to the activation controlled region [1]. The technologically feasible potentials for DMFCs are normally 0.4~0.5 V [3].

Figure 3 showed typical curves of the $Pt_{77}Ru_{23}$/CNT catalyst. The current densities gradually decayed with time and the decline in the oxidation currents is different for each catalyst at each temperature. Apparently, the deactivation of the catalysts proceeded very rapidly over the initial period of several minutes. After that, a slower steady decay was observed. The continuous current decay is indicative of a loss in the catalytic activity. Two factors may lead to the catalyst deactivation. One is the oxidation of the Ru surface [43,44], forming oxides such as RuO_2 and RuO_3 that are not active for CO oxidation. This is a reversible process. The other is the blockage of the active sites by adsorbed organic residues from methanol oxidation that are formed slowly and can only be oxidized at high anodic potentials. Gasteiger *et al.* reported that long-duration experiments with smooth electrodes are very sensitive to the effect of surface-active impurities [8]. They found that 0.1 ppm of any surface-active impurities in the electrolyte would deactivate ~7% of the catalyst surface in 10 min after its immersion and an additional ~3% for each of the following 10 min interval [8].

The turn over number (TON) and the activation energy for each catalyst were calculated from the experimental data. The TON, which is defined as the number of methanol molecules that react per catalyst surface site per second, directly reflects the steady-state current density for methanol electro-oxidation; its value can be calculated from [43,45]:

$$TON\left[\frac{molecules}{s\cdot site}\right]=\frac{I[mA\cdot cm^{-2}]\times N_A}{nF\times m(Pt)[cm^{-2}]} \quad (4)$$

where I is the steady-state current density, n the number of electrons produced by oxidation of 1 mol methanol, F the Faraday constant, m(Pt) the mean atomic density of surface platinum on Pt(111) (1.51×10^{15} cm^{-2}), N_A the Avogadro constant, and surface area of the catalysts has been reported in our previous study [24].

Figure 3. Chronoamperometry performed for methanol electro-oxidation on $Pt_{77}Ru_{23}$/CNT at different temperatures. The applied potentials are (a) 0.4 V and (b) 0.5 V.

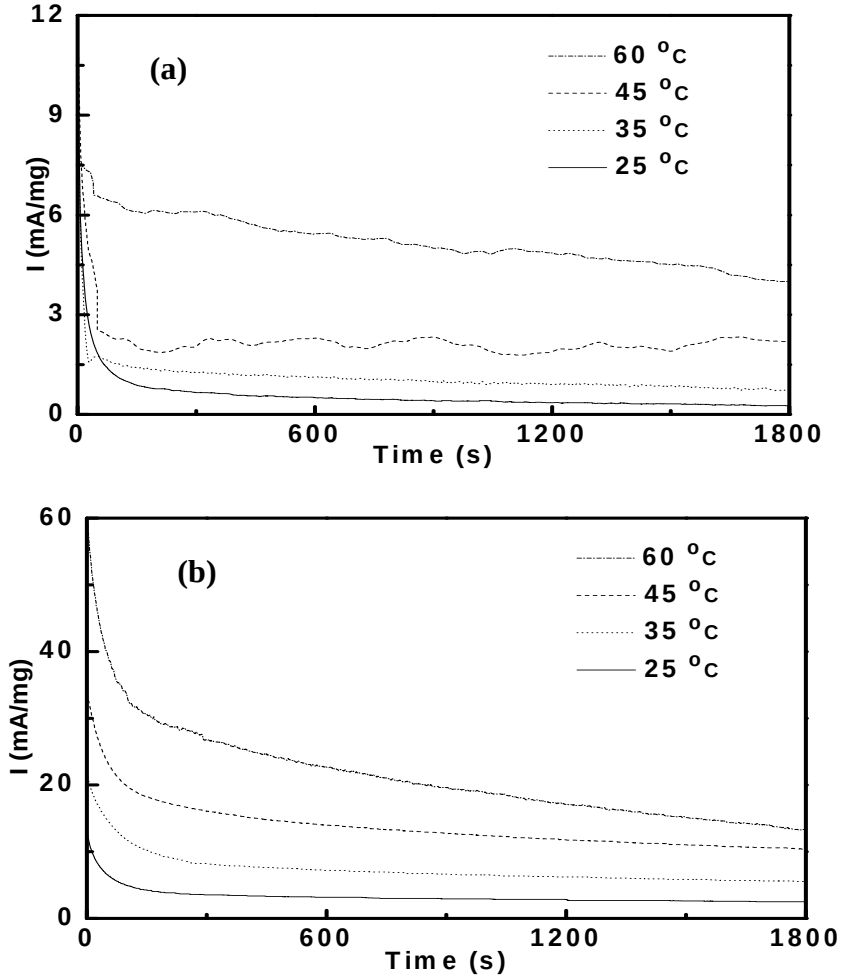

The results of TON for methanol electro-oxidation in 1.0 M H_2SO_4 + 2.0 M CH_3OH at different potentials were listed in Table 2. The TONs were found to be different for different catalysts and dependent on the applied potentials and temperatures. For example, the TONs of $Pt_{53}Ru_{47}$/CNT and $Pt_{69}Ru_{31}$/CNT at 0.4 V and 25 ºC are 0.93×10^{-3} and 0.28×10^{-3} s^{-1}, respectively, while that of $Pt_{77}Ru_{23}$/CNT is 0.53×10^{-3} s^{-1}. In addition, TON was found to increase with the increase of applied potentials and temperatures, which can be clearly seen from the data in Table 2. It can be also seen that $Pt_{53}Ru_{47}$/CNT has the largest TON at each potential and temperature, meaning that it is able to catalyze more methanol in the same period using the same number of sites than the other two catalysts. Therefore, on this measure, the $Pt_{53}Ru_{47}$/CNT catalyst has the best catalytic activity toward electro-oxidation of methanol, consistent with the conclusions obtained from Figure 1(b) and that reported in our previous paper [24].

Table 2. Turnover number (molecule s^{-1} $site^{-1} \times 10^{-3}$) of PtRu/CNT catalysts for methanol electro-oxidation at different potentials.

Catalysts	Applied potentials							
	0.4 V				0.5 V			
	25 ºC	35 ºC	45 ºC	60 ºC	25 ºC	35 ºC	45 ºC	60 ºC
$Pt_{53}Ru_{47}$/CNT	0.93	1.64	2.64	5.52	4.60	6.98	13.3	26.3
$Pt_{69}Ru_{31}$/CNT	0.28	0.49	0.88	1.98	2.03	3.73	6.27	14.5
$Pt_{77}Ru_{23}$/CNT	0.53	0.97	1.71	3.38	3.05	5.70	9.95	19.6

Figure 4 shows the Arrhenius plots for the catalysts, plots of the logarithm of the current density (ln (*I*)) *vs.* the inverse temperature (1/*T*). The activation energies (E_a) were obtained from the slopes of the curves at a particular potential by fitting the Arrhenius equation:

$$slope = \frac{\partial \ln(I)}{\partial (1/T)} = -\frac{E_a}{R} \quad (5)$$

where *R* is the gas constant. Linear relationships between ln(*I*) and 1/*T* were observed in all cases, indicating that the reaction mechanism at both potentials was not changed with the temperatures. The apparent activation energy listed in Table 3 for each catalyst was obtained from the parallel lines according to Equation 5.

Figure 4. Arrhenius plots of the PtRu/CNT catalysts at different potentials, (—) 0.4 V and (—) 0.5 V.

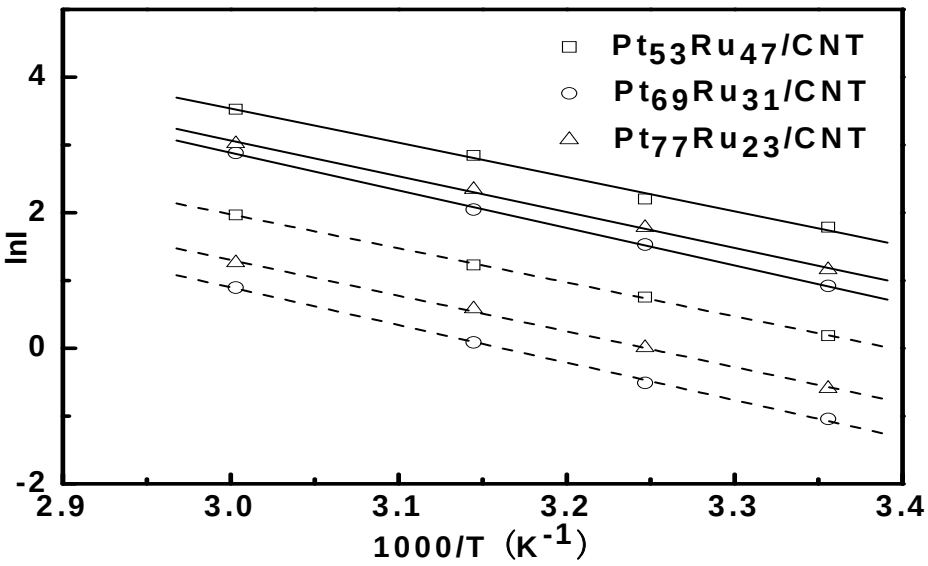

Table 3. Activation energy of the PtRu/CNT catalysts in methanol electro-oxidation.

Catalysts	Activation energy (kJ/mol)
$Pt_{53}Ru_{47}$/CNT	41.9 ± 0.3
$Pt_{69}Ru_{31}$/CNT	46.0 ± 0.1
$Pt_{77}Ru_{23}$/CNT	43.8 ± 0.1

The activation energy for methanol electro-oxidation strongly depends on a catalytic reaction system. Significantly different values were reported in the literature for Pt-Ru alloy electrodes, from 55 kJ/mol for unsupported PtRu catalyst [1] to 95 kJ/mol in 2 M CH_3OH and 1 M H_2SO_4 [46] at 0.4 V, and from 60 kJ/mol for PtRu alloy with 46 at.% of Ru [8] to 65 kJ/mol for PtRu particles incorporated in a Nafion membrane [39]. The electrolyte concentrations can also strongly influence the measured current densities [47]. Variations in methanol concentrations, surface compositions, and even the synthesis methods can lead to the different values observed. High activation energy values mean that there is a need for high operation temperatures of DMFCs.

Although different results of activation energy for methanol electro-oxidation have been reported, the activation energies we obtained for the PtRu/CNT catalysts are much lower (Table 3). Several possible factors may contribute to the observed enhancement of electro-oxidation on these PtRu/CNT catalysts; they may include particle size, compositions, and crystalline structures of the alloy catalysts [24]. However, the CNT catalyst support could be an important factor affecting the catalyst activity due to metal-support interactions. In a previous study, fullerene soot and carbon black were found to have different interactions with the Pt/Ru catalysts [48] due to their different surface structures. Although the enhancement from the metal-carbon support interactions toward methanol electro-oxidation is not fully understood, we believe that the CNTs, which have a curved graphitic surface, could promote the PtRu activity.

According to the methanol electro-oxidation mechanism, dehydrogenation of methanol to methanolic CO (Equation 1) does not require participation of oxygen-containing species to complete. However, methanolic CO oxidation to CO_2 requires extra oxygen to go to completion (Equation 3). The oxygen-containing species can only come from water discharging, including interfacial or near surface bulk water molecules (Equation 2) [49]. Tang *et al.* [50] reported that H_2O molecules prefer to be adsorbed on CNTs when CNTs are positively charged. For high-density H_2O adsorbed on the outer walls of CNTs, more H_2O molecules at interface or near surface bulk can serve as electron donors. Therefore, the CNT support may have assisted water discharging on the Ru sites that in turn leads to increased OH_{ads} and enhanced CO removal.

3.4. Reaction Orders in Methanol Electro-Oxidation

Figure 5 shows a comparison of the methanol electro-oxidation rates on $Pt_{77}Ru_{23}$/CNT at 35 ºC at different methanol concentrations from 0.02 to 2.0 M. As can be seen, the current densities increase with increasing methanol concentrations. On the basis of the above examination of the interactions of methanol and PtRu/CNT, we can determine the rate-determining step (RDS) for methanol electro-

oxidation. Since we are concerned about the long-term activity of the PtRu/CNT catalysts, we will focus on the overall process rather than individual steps.

Figure 5. Chronoamperometry collected for methanol electro-oxidation on $Pt_{77}Ru_{23}$/CNT with different methanol concentrations in 1.0 M H_2SO_4 at 35 ºC. The applied potential is 0.5 V.

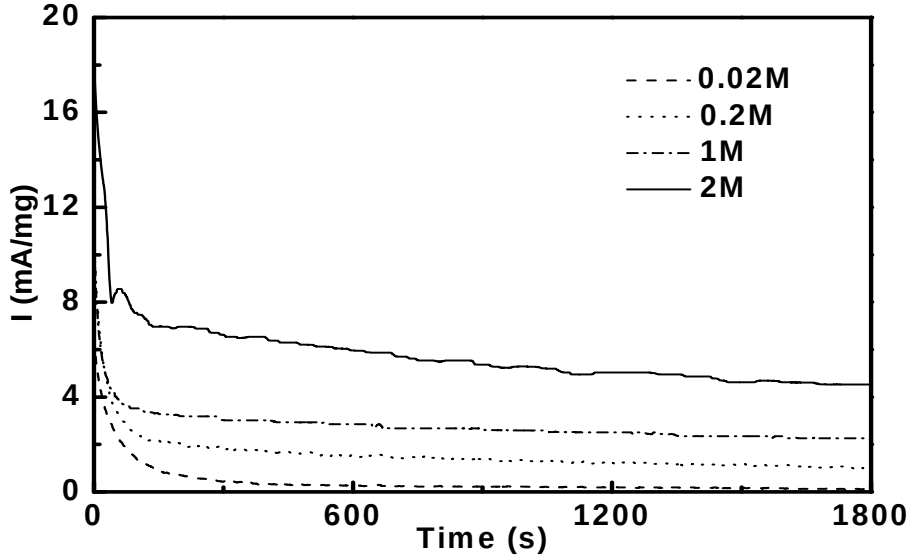

The overall oxidation current density can be written as [51],

$$I = nFkC^{m} \quad (6)$$

where k is the reaction rate constant, C the concentration of methanol, and m the apparent reaction order. Therefore, the slope of log(I) *vs.* log(C) plot at a constant potential will give the apparent reaction order (m). Using the steady-state current densities, a typical plot for methanol electro-oxidation at 35 ºC at a potential of 0.5 V is presented in Figure 6. The straight line with a slope of 0.5 implies that methanol electro-oxidation follows half-order kinetics with respect to methanol concentrations. The same value was reported for unsupported Pt-Ru catalysts [35] as well as for Pt-Ru supported on carbon black [52,53].

Franaszczuk *et al.* [54] have shown that the RDS in methanol electro-oxidation is the initial C-H bond splitting of a methyl, *i.e.* the initial dehydrogenation of methanol, on a millisecond time scale. However, on the time scale of one thousand seconds, the oxidation currents have decayed by almost one order of magnitude, indicating a change in the RDS due to the accumulation of methanolic residues on the catalyst surface. Gasteiger *et al.* found that sputtered Pt-Ru alloys with rich Ru yielded methanol concentration dependent electro-oxidation rates [30]. They also reported that pure Pt surface showed a relatively weak dependence on methanol concentrations and the apparent reaction order with respect to methanol is close to zero. In the latter case, the RDS is the oxidative removal of methanol dehydrogenation fragments. In contrast, on Ru-rich alloy surfaces, the overall methanol electro-oxidation rate at steady state is mainly limited by the reduction rate of methanol adsorption, which

explains the dependency of electro-oxidation rate on methanol concentrations for our Pt-Ru/CNT catalysts at steady-state.

Figure 6. Reaction rate (current density) of methanol electro-oxidation on $Pt_{77}Ru_{23}$/CNT as a function of methanol concentrations in 1.0 M H_2SO_4 at 35 ºC with applied potential at 0.5 V.

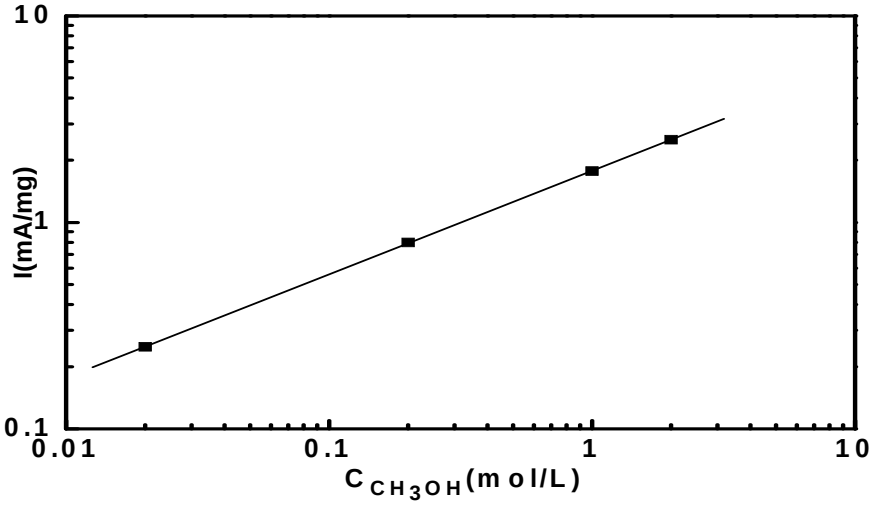

4. Conclusions

The kinetics of methanol electro-oxidation on CNT-supported Pt-Ru alloy nanoparticles was investigated in H_2SO_4 + CH_3OH electrolyte solutions. Results of cyclic voltammetry at different temperatures showed that methanol electro-oxidation is very sensitive to the changes in temperatures. However, close values of Tafel slope at different temperatures were observed for all catalysts indicating that the reaction mechanism is similar for the catalysts with different atomic ratios of Pt and Ru within the experimental temperature range. The onset potentials of methanol electro-oxidation shifted negatively at high temperatures. Linear relationships between logarithm of the current densities and the inverse temperatures were observed. Activation energies were obtained from the corresponding Arrhenius plots. The activation energies were found to be much lower on the PtRu/CNT catalysts than those reported in the literature, which was attributed to the metal support interactions between PtRu nanoparticles and CNT. The electro-oxidation of methanol on the PtRu catalysts was found to follow half-order kinetics with respect to the methanol concentrations.

Acknowledgements

This work is partially supported by the National Science Foundation through grant DMI-0522931 and the Missouri University of Science and Technology.

References and Notes

1. Vidakovic, T.; Christov, M.; Sundmacher, K. Rate expression for electrochemical oxidation of methanol on a direct methanol fuel cell anode. *J. Electroanal. Chem.* **2005**, *580*, 105-121.

2. Kabbabi, A.; Durand, R.; Beden, B.; Hahn, F.; Leger, J.M.; Lamy, C. In situ FTIRS study of the electrocatalytic oxidation of carbon monoxide and methanol at platinum–ruthenium bulk alloy electrodes. *J. Electroanal. Chem.* **1998**, *444*, 41-53.
3. Jusys, Z.; Kaiser, J.; Behm, R.J. Composition and activity of high surface area PtRu catalysts towards adsorbed CO and methanol electrooxidation: A DEMS study. *Electrochim. Acta* **2002**, *47*, 3693-3706.
4. Laborde, H.; Leger, J.M.; Lamy, C. Electrocatalytic oxidation of methanol and C1 molecules on highly dispersed electrodes Part II: Platinum-ruthenium in polyaniline. *J. Appl. Electrochem.* **1994**, *24*, 1019-1027.
5. Bagotzsky, V.S.; Vassiliev, Y.B.; Khazova, O.A. Generalized scheme of chemisorption, electrooxidation and electroreduction of simple organic compounds on platinum group metals. *J. Electroanal. Chem.* **1977**, *81*, 229.
6. Bockris, J.O'M.; Wroblowa, H. Electrocatalysis. *J. Electroanal. Chem. Interfacial Electrochem.* **1964**, *7*, 428.
7. Watanabe, M.; Motoo, S. Electrocatalysis by ad-atoms: Part II. Enhancement of the oxidation of methanol on platinum by ruthenium ad-atoms. *J. Electroanal. Chem. Interfacial Electrochem.* **1975**, *60*, 267.
8. Gasteiger, H.A.; Markovic, N.; Ross, P.N.; Cairns, E.J. Temperature-dependent methanol electro-oxidation on well-characterized Pt-Ru alloys. *J. Electrochem. Soc.* **1994**, *141*, 1795-1803.
9. Takasu, Y.; Fujiwara, T.; Murakami, Y.; Sasaki, K.; Oguri, M.; Asaki, T.; Sugimoto, W. Effect of structure of carbon-supported PtRu electrocatalysts on the electrochemical oxidation of methanol. *J. Electrochem. Soc.* **2000**, *147*, 4421-4427.
10. Goodenough, J.B.; Manohara, R.; Shukla, A.K.; Ramesh, K.V. Intraalloy electron transfer and catalyst performance: a spectroscopic and electrochemical study. *Chem. Mater.* **1989**, *1*, 391-398.
11. Hamnett, A. Mechanism and electrocatalysis in the direct methanol fuel cell. *Catal. Today* **1997**, *38*, 445-457.
12. Liu, R.; Iddir, H.; Fan, Q.; Hou, G.; Bo, A.; Ley, K.L.; Smotkin, E.S.; Sung, Y.E.; Kim, H.; Thomas, S.; Wieckowski, A. Potential-dependent infrared absorption spectroscopy of adsorbed CO and X-ray photoelectron spectroscopy of arc-melted single-phase Pt, PtRu, PtOs, PtRuOs, and Ru electrodes. *J. Phys. Chem.B.* **2000**, *104*, 3518-3531.
13. Waszczuk, P.; Wieckowski, A.; Zelenay, P.; Gottesfeld, S.; Coutanceau, C.; Leger, J.M.; Lamy, C. Adsorption of CO poison on fuel cell nanoparticle electrodes from methanol solutions: a radioactive labeling study. *J. Electroanal. Chem.* **2001**, *511*, 55-64.
14. Che, G.; Lakshmi, B.B.; Martin, C.R.; Fisher, E.R. Metal-nanocluster-filled carbon nanotubes: catalytic properties and possible applications in electrochemical energy storage and production. *Langmuir* **1999**, *15*, 750-758.
15. Li, W.; Liang, C.; Qiu, J.; Zhou, W.; Han, H.; Wei, Z.; Sun, G.; Xin, Q. Carbon nanotubes as support for cathode catalyst of a direct methanol fuel cell. *Carbon* **2002**, *40*, 791-794.
16. Xing, Y. Synthesis and electrochemical characterization of uniformly-dispersed high loading Pt nanoparticles on sonochemically-treated carbon nanotubes. *J. Phys. Chem. B* **2004**, *108*, 19255-19259.

17. Wang, X.; Waje, M.; Yan, Y. CNT-based electrodes with high efficiency for proton exchange membrane fuel cells. *Electrochem. Solid State Lett.* **2004**, *8*, A42-A44.
18. Liu, Z.L.; Lee, J.Y.; Chen, W.; Han, M.; Gan, L.M. Physical and electrochemical characterizations of microwave-assisted polyol preparation of carbon-supported PtRu nanoparticles. *Langmuir* **2004**, *20*, 181-187.
19. Park, K.W.; Sung, Y.E.; Han, S.; Yun, Y.; Hyeon, T. Origin of the enhanced catalytic activity of carbon nanocoil-supported PtRu alloy electrocatalysts. *J. Phys. Chem. B* **2004**, *108*, 939-944.
20. Lin, Y.; Cui, X.; Yen, C.H.; Wai, C.M. PtRu/Carbon nanotube nanocomposite synthesized in supercritical fluid: a novel electrocatalyst for direct methanol fuel cell. *Langmuir* **2005**, *21*, 11474-11479.
21. Frackowiak, E.; Lota, G.; Cacciaguerra, T.; Beguin, F. Carbon nanotubes with Pt–Ru catalyst for methanol fuel cell. *Electrochem. Comm.* **2006**, *8*, 129-132.
22. Girishkumar, G.; Hall, T.D.; Vinodgopal, K.; Kamat, P.V. Single wall carbon nanotube supports for portable direct methanol fuel cells. *J. Phys. Chem. B* **2006**, *110*, 107-114.
23. Li, W.; Wang, X.; Chen, Z.; Waje, M.; Yan, Y. Pt−Ru supported on double-walled carbon nanotubes as high-performance anode catalysts for direct methanol fuel cells. *J. Phys. Chem. B* **2006**, *110*, 15353-15358.
24. Li, L.; Xing, Y. Pt−Ru nanoparticles supported on carbon nanotubes as methanol fuel cell catalysts. *J. Phys. Chem. C* **2007**, *111*, 2803-2808.
25. Yu, W.Y.; Tu, W.X.; Liu, H.F. Synthesis of nanoscale platinum colloids by microwave dielectric heating. *Langmuir* **1999**, *15*, 6-9.
26. Li, W.; Liang, C.; Zhou, W.; Qiu, J.; Zhou, Z.; Han, H.; Wei, Z.; Sun, G.; Xin, Q. Preparation and characterization of multiwalled carbon nanotube-supported platinum for cathode catalysts of direct methanol fuel cells. *J. Phys. Chem. B* **2003**, *107*, 6292-6299.
27. Xing, Y.; Li, L.; Chusuei, C.C.; Hull, R.V. Sonochemical oxidation of multiwalled carbon nanotubes. *Langmuir* **2005**, *21*, 4185-4190.
28. Schmidt, T.J.; Gasteiger, H.A.; Stab, G.D.; Urban, P.M.; Kolb, D.M.; Behm, R.J. Characterization of high-surface-area electrocatalysts using a rotating disk electrode configuration. *J. Electrochem. Soc.* **1998**, *145*, 2354-2358.
29. Arico, A.S.; Baglio, V.; Blasi, A.D.; Modica, E.; Antonucci, P.L.; Antonucci, V. Analysis of the high-temperature methanol oxidation behaviour at carbon-supported Pt–Ru catalysts. *J. Electroanal. Chem.* **2003**, *557*, 167-176.
30. Gasteiger, H.A.; Markovic, N.; Ross, P.N.; Cairns, E.J. Methanol electrooxidation on well-characterized platinum-ruthenium bulk alloys. *J. Phys. Chem.* **1993**, *97*, 12020-12029.
31. Kauranen, P.; Skou, E.; Munk, J. Kinetics of methanol oxidation on carbon-supported Pt and Pt + Ru catalysts. *J. Electroanal. Chem.* **1996**, *404*, 1-13.
32. Ticanelli, E.; Beery, T.G.; Paffett, M.T.; Gottesfeld, S. An electrochemical, ellipsometric, and surface science investigation of the PtRu bulk alloy surface. *J. Electroanal. Chem.* **1989**, *258*, 61-77.
33. Choi, J.H.; Park, K.W.; Kwon, B.K.; Sung, Y.E. Methanol oxidation on Pt/Ru, Pt/Ni, and Pt/Ru/Ni anode electrocatalysts at different temperatures for DMFCs. *J. Electrochem. Soc*. **2003**, *150*, A973-A978.

34. Raicheva, S.N.; Christov, M.V.; Sokolova, E.I. Effect of the temperature on the electrochemical behaviour of aliphatic alcohols. *Electrochim. Acta* **1981**, *26*, 1669-1676.
35. Chu, D.; Gilman, S. Methanol electro-oxidation on unsupported Pt-Ru alloys at different temperatures. *J. Electrochem. Soc.* **1996**, *143*, 1685-1690.
36. Madey, T.E.; Engelhardt, H.A.; Menzel, D. Adsorption of oxygen and oxidation of CO on the ruthenium (001) surface. *Surf. Sci.* **1975**, *48*, 304-328.
37. Vidakovic, T.; Christov, M.; Sundmacher, K.; Nagabhushana, K.S.; Fei, W.; Kinge, S.; Bonnemann, H. PtRu colloidal catalysts: Characterisation and determination of kinetics for methanol oxidation. *Electrochim. Acta* **2007**, *52*, 2277-2284.
38. Roth, C.; Marty, N.; Hahn, F.; Leger, J.M.; Lamy, C.; Fuess, H. Characterization of differently synthesized Pt-Ru fuel cell catalysts by cyclic voltammetry, FTIR spectroscopy, and in single cells. *J. Electrochem. Soc.* **2002**, *149*, E433-E439.
39. Meli, G.; Leger, J.M.; Lamy, C. Direct electrooxidation of methanol on highly dispersed platinum-based catalyst electrodes: temperature effect. *J. Appl. Electrochem.* **1993**, *23*, 197-202.
41. Schmidt, T.J.; Gasteiger, H.A.; Behm, R.J. Methanol electrooxidation on a colloidal PtRu-alloy fuel-cell catalyst. *Electrochem. Commun.* **1999**, *1*, 1-4.
42. Chrzanowski, W.; Wieckowski, A. Surface structure effects in Platinum/Ruthenium methanol oxidation electrocatalysis. *Langmuir* **1998**, *14*, 1967-1970.
43. Herrero, E.; Franaszczuk, K.; Wieckowski, A. Electrochemistry of methanol at low index crystal planes of platinum: an integrated voltammetric and chronoamperometric study. *J. Phys. Chem.* **1994**, *98*, 5074-5083.
44. Hoster, H.; Iwasita, T.; Baumgartner, H.; Vielstich, W. Pt–Ru model catalysts for anodic methanol oxidation: Influence of structure and composition on the reactivity. *Phys. Chem. Chem. Phys.* **2001**, *3*, 337-346.
45. Chrzanowski, W.; Kim, H.; Wieckowski, A. Enhancement in methanol oxidation by spontaneously deposited ruthenium on low-index platinum electrodes. *Catal. Lett.* **1998**, *50*, 69-75.
46. Entina, V.S.; Petri, O.A. Electrooxidation of methanol on Pt-Ru and Ru electrodes at different temperatures. *Elektrokhimiya* **1968**, *4*, 678.
47. McNicol, B.D. Electrocatalytic problems associated with the development of direct methanol-air fuel cells. *J. Electroanal. Chem.* **1981**, *118*, 71-87.
48. Hills, C.W.; Nashner, M.S.; Frenkel, A.I.; Shapley, J.R.; Nuzzo, R.G. Carbon support effects on bimetallic Pt−Ru nanoparticles formed from molecular precursors. *Langmuir* **1999**, *15*, 690-700.
49. Capon, A.; Parsons, R. The oxidation of formic acid at noble metal electrodes Part III. Intermediates and mechanism on platinum electrodes. *J. Electroanal. Chem.* **1973**, *45*, 205.
50. Tang, D.; Ci, L.; Zhou, W.; Xie, S. Effect of H_2O adsorption on the electrical transport properties of double-walled carbon nanotubes. *Carbon* **2006**, *44*, 2155-2159.
51. Bard, A.J.; Faulkner, L.R. *Electrochemical Methods Fundamentals and Applications*, 2nd ed.; John Wiley: New York, NY, USA, 2001.
52. Tripkovic, A.V.; Popovic, K.D.; Lovic, J.D. Kinetic study of methanol oxidation on Pt_2Ru_3/C catalyst in alkaline media. *J. Serb. Chem. Soc.* **2007**, *72*, 1095-1101.

53. Gojkovic, S.L.; Vidakovic, T.R.; Durovic, D.R. Kinetic study of methanol oxidation on carbon-supported PtRu electrocatalyst. *Electrochim. Acta* **2003**, *48*, 3607-3614.
54. Franaszczuk, K.; Herrero, E.; Zelenay, P.; Wieckowski, A.; Wang, J.; Masel, R.I. A comparison of electrochemical and gas-phase decomposition of methanol on platinum surfaces. *J. Phys. Chem.* **1992**, *96*, 8509-8516.